6-13-2017

Presurgical thalamic "hubness" predicts surgical outcome in temporal lobe epilepsy.

Xiaosong He
Thomas Jefferson University

Gaelle E. Doucet
Icahn School of Medicine at Mount Sinai

Dorian Pustina
University of Pennsylvania

Michael R. Sperling
Thomas Jefferson University

Ashwini D. Sharan
Thomas Jefferson University

Authors
Xiaosong He, Gaelle E. Doucet, Dorian Pustina, Michael R. Sperling, Ashwini D. Sharan, and Joseph I. Tracy

Published Ahead of Print on May 17, 2017 as 10.1212/WNL.0000000000004035

Presurgical thalamic "hubness" predicts surgical outcome in temporal lobe epilepsy

Xiaosong He, PhD
Gaelle E. Doucet, PhD
Dorian Pustina, PhD
Michael R. Sperling, MD
Ashwini D. Sharan, MD
Joseph I. Tracy, PhD

Correspondence to Dr. Tracy: Joseph.Tracy@jefferson.edu

ABSTRACT

Objective: To characterize the presurgical brain functional architecture presented in patients with temporal lobe epilepsy (TLE) using graph theoretical measures of resting-state fMRI data and to test its association with surgical outcome.

Methods: Fifty-six unilateral patients with TLE, who subsequently underwent anterior temporal lobectomy and were classified as obtaining a seizure-free (Engel class I, n = 35) vs not seizure-free (Engel classes II–IV, n = 21) outcome at 1 year after surgery, and 28 matched healthy controls were enrolled. On the basis of their presurgical resting-state functional connectivity, network properties, including nodal hubness (importance of a node to the network; degree, betweenness, and eigenvector centralities) and integration (global efficiency), were estimated and compared across our experimental groups. Cross-validations with support vector machine (SVM) were used to examine whether selective nodal hubness exceeded standard clinical characteristics in outcome prediction.

Results: Compared to the seizure-free patients and healthy controls, the not seizure-free patients displayed a specific increase in nodal hubness (degree and eigenvector centralities) involving both the ipsilateral and contralateral thalami, contributed by an increase in the number of connections to regions distributed mostly in the contralateral hemisphere. Simulating removal of thalamus reduced network integration more dramatically in not seizure-free patients. Lastly, SVM models built on these thalamic hubness measures produced 76% prediction accuracy, while models built with standard clinical variables yielded only 58% accuracy (both were cross-validated).

Conclusions: A thalamic network associated with seizure recurrence may already be established presurgically. Thalamic hubness can serve as a potential biomarker of surgical outcome, outperforming the clinical characteristics commonly used in epilepsy surgery centers. ***Neurology*® 2017;88:1–9**

GLOSSARY

ATL = anterior temporal lobectomy; **BC** = betweenness centrality; **DC** = degree centrality; **DSM-IV** = Diagnostic and Statistical Manual of Mental Disorders, 4th edition; **EC** = eigenvector centrality; $\mathbf{E_{global}}$ = global efficiency; **FDR** = false discovery rate; **HC** = healthy control; **MST** = minimum spanning tree; **NSF** = not seizure-free; **rsFC** = resting-state functional connectivity; **rsfMRI** = resting-state fMRI; **SANTE** = Stimulation of the Anterior Nucleus of Thalamus for Epilepsy; **SF** = seizure-free; **SVM** = support vector machine; **TLE** = temporal lobe epilepsy.

Anterior temporal lobectomy (ATL) is the most common resective surgery for drug-resistant temporal lobe epilepsy (TLE). However, the postoperative seizure freedom (with or without isolated auras) rate is only between 48% and 76%[1–5] at 1 year, dropping to <50% after 10 years.[6] A hypothesis underlying surgical failure is that an occult epileptogenic network, potentially composed of extratemporal regions, is already established preoperatively and spared during surgery, later providing support for seizure recurrence.[7]

Nodes of such a network may include the contralateral hippocampus,[8] frontal lobe,[9,10] parietal lobe,[10] anterior cingulate,[10] insula,[10] and thalamus,[8,11] where regional structural abnormalities and aberrant ictal-temporal structural connections (frontal lobe, insula, and thalamus)[12,13] were associated with unfavorable outcome in TLE. To optimize surgical outcomes,

Editorial, page 2246

Supplemental data at Neurology.org

From the Departments of Neurology (X.H., M.R.S., J.I.T.) and Neurosurgery (A.D.S.), Thomas Jefferson University, Philadelphia, PA; Department of Psychiatry (G.E.D.), Icahn School of Medicine at Mount Sinai, New York, NY; and Departments of Neurology and Radiology (D.P.), University of Pennsylvania, Philadelphia.

Go to Neurology.org for full disclosures. Funding information and disclosures deemed relevant by the authors, if any, are provided at the end of the article.

the disruption of this network appears critical, posing a challenge to understand its organization and, in particular, to articulate its core node(s) before surgery. These nodes can serve as potential targets for alternative treatments (e.g., brain electric stimulation), eventually benefiting patients who might fail ATL.

Resting-state functional connectivity (rsFC), a measure of intrinsic functional organization,[14] offers an alternative perspective of preoperative reorganization associated with seizure recurrence. Accordingly, we use graph theory to investigate the presurgical rsFC in patients with unilateral TLE who subsequently underwent ATL. We hypothesize that nodal hubness, a measure quantifying the importance of a node to network organization,[15] will identify core nodes of the aforementioned network(s). We then test, through support vector machine (SVM) learning, the value of this presurgical nodal information for the goal of predicting seizure outcome.

METHODS

Participants. Fifty-six patients with refractory unilateral TLE were recruited from the Thomas Jefferson Comprehensive Epilepsy Center. Candidacy for surgery was determined by a multimodal evaluation including neurologic history and examination, scalp video-EEG, MRI, PET, and neuropsychological testing.[1] Patients were excluded for any of the following reasons: previous brain surgery, medical illness with the CNS other than epilepsy, extratemporal or multifocal epilepsy, contraindications to MRI, or diagnosis/hospitalization for any Axis I disorder listed in the DSM-IV. Depressive disorders were allowed, given the high comorbidity with epilepsy.[16] All patients underwent a standard *en bloc* ATL to remove their epileptogenic temporal lobe. None of the patients had intraoperative or perioperative complications, and the preoperative antiepileptic regimen was continued for all patients in the postoperative period, with reduction of dosage in a few cases because of their seizure freedom.

Seizure outcome was assessed 1 year after surgery. Thirty-five patients meeting criteria for Engel class I[17] (seizure free with or without auras) were classified as seizure-free (SF). Twenty-one patients who met criteria for Engel class II, III, or IV[17] (one or more recurrent complex partial or secondarily generalized seizures) were classified as not SF (NSF). The demographic and clinical characteristics of the final experimental groups are presented in table 1, along with demographic information for 28 matched healthy controls (HCs). All HCs were free of psychiatric or neurologic disorders on the basis of a health screening measure.

Standard protocol approvals, registrations, and patient consents. This study was approved by the Institutional Review Board for Research With Human Subjects at Thomas Jefferson University. All participants provided a written informed consent.

MRI acquisition, data preprocessing, network construction, and graph theoretical parameter estimation. T1-weighted structural imaging and 5-minute resting-state fMRI (rsfMRI) data were obtained from all the participants. The methodological details regarding MRI acquisition, data preprocessing, network construction, and graph theoretical parameters estimation are described in the e-Methods at Neurology.org. Briefly, regional parcellation was applied on the preprocessed rsfMRI data with the Automated Anatomical Labeling template (45 nodes per hemisphere).[18] The maximal overlap discrete wavelet transform[19] was performed to extract information in the frequency interval of ≈0.05 to 0.1 Hz (scale 2).[20] The pairwise interregional wavelet correlation coefficients, later defined as edges, were estimated to generate a wavelet correlation matrix for each participant. Next, we used a minimum spanning tree (MST) method[21] to build individual binary undirected graphs. On the basis of the correlation matrices (absolute value), we first defined the MST that connected all 90 regional nodes with 89 edges, completed for every participant. Additional edges were then added to the MST in the descending order of the wavelet correlation,[20] yielding a series of networks with connection density ranging from 5% to 50% in increments of 1%.[21] For every node at every density, 3 hubness measures were estimated: degree centrality (DC; richness of connections), betweenness centrality (BC; importance for mediating signals between other nodes), and eigenvector centrality (EC; influence of a node in a network).[22] Global efficiency (E_{global}), as a measure of network integration,[22] was also estimated to test the deleterious influence of certain nodes on full-brain functional organization. As validation, we also report findings produced by a different parcellation scheme (Harvard-Oxford Atlas,[23] 112 nodes) or weighted graphs as supplementary results.

Statistical analysis. Group-level comparisons of demographic and clinical characteristics were carried out with independent-sample t tests, one-way analysis of variance, or χ^2 tests, as appropriate, with IBM SPSS version 22.

To assess group differences in hubness measures and E_{global}, the Welch permutation t test was used. Welch t statistics was chosen to account for the unequal sample size and variance, with the permutation used to estimate the probability of significant group differences without assuming a normal distribution. For every comparison of every measure at each density, 10,000 permutations were performed by randomly relabeling the 2 groups, yielding a permuted t statistic distribution from which the p values associated with observed t statistics could be estimated. Comparisons between patients (SF and NSF) and HCs were carried out in the same manner. Multiple comparisons were corrected with the false discovery rate (FDR) in all reported results unless otherwise noted.

For nodes with hubness measures that yielded a significant difference in seizure outcome, we carried out 3 additional independent analyses to determine the network features contributing to this difference:

1. We examined the effect of removing such node(s) and associated edges to the integration of the full network. To do this, we tested for change (before vs after removal) in E_{global} across groups. Accordingly, a higher reduction in E_{global} indicates greater importance.
2. For nodes outside the ictal-temporal lobe associated with outcome, we reanalyzed and compared their hubness values after removing all nodes/edges involving the ictal-temporal lobe (8 nodes: hippocampus, parahippocampus, amygdala, middle and superior temporal pole, and inferior, middle, and superior temporal lobed). This manipulation allowed us to determine whether any hubness difference observed between the outcome groups was dependent on the ictal-temporal lobe.

Table 1 Sample demographic and clinical characteristics

Sample group	SF TLE (n = 35)	NSF TLE (n = 21)	HCs (n = 28)	$F/t/\chi^2$ value	*p* Value
Epileptogenic temporal lobe (L/R), n	18/17	8/13	NA	0.94	0.33
Age, mean ± SD, y	41.25 ± 12.60	38.58 ± 13.25	38.84 ± 12.62	0.40	0.67
Sex (M/F), n	21/14	9/12	14/14	1.64	0.44
Handedness (R/L), n	30/5	14/7	23/5	3.10	0.21
Verbal IQ[a]	96.18 ± 14.22	93.29 ± 15.36	NA	0.71	0.48
Performance IQ[a]	94.88 ± 10.41	96.19 ± 17.58	NA	−0.31	0.76
Full-scale IQ[a]	95.29 ± 10.31	93.86 ± 17.10	NA	0.35	0.73
Age at epilepsy onset, mean ± SD, y	23.73 ± 12.60	21.55 ± 10.87	NA	0.66	0.51
Duration of epilepsy, mean ± SD, y	17.52 ± 14.53	17.03 ± 11.21	NA	0.14	0.89
Seizure focality (with/without GS or 2nd GS), n	15/20	10/11	NA	0.12	0.73
Interictal spike (ipsilateral/bilateral), n	29/6	15/6	NA	1.02	0.31
Preoperative intracranial EEG recording (Y/N), n	8/27	9/12	NA	2.48	0.12
Temporal pathology (NB/HS/T/E/D), n	14/15/4/1/1	13/5/2/1/0	NA	2.71	0.26
Seizure type, n			NA		
SPS	1				
CPS	12	8			
CPS/SPS	2	2			
SPS + 2nd GS		1			
CPS + 2nd GS	9	3			
CPS/SPS + 2nd GS	3	1			
CPS + GS	4	4			
CPS/SPS + GS	3	2			
GS	1				

Abbreviations: CPS = complex partial seizure; D = dysplasia; E = encephalocele; GS = generalized tonic-clonic seizure; HC = healthy control; HS = hippocampal sclerosis; NB = normal brain; NSF = not seizure-free; 2nd GS = secondary generalized tonic-clonic seizure; SF = seizure-free; SPS = simple partial seizure; T = tumor; TLE = temporal lobe epilepsy.
Temporal pathology was diagnosed by neuroradiologists from presurgical MRI scans. χ^2 test performed with NB, HS, and others (T, E, and D together). For continuous variables, independent-sample *t* tests or one-way analysis of variance was carried out, as appropriate. For categorical variables, χ^2 tests were carried out.
[a] One SF patient did not have valid IQ scores.

3. For each node demonstrating a group difference in outcome, we analyzed connectivity with the other 89 nodes of the whole-brain matrix. Binary matrices across different densities were used, coding edges as either 1 (present) or 0 (absent). The χ^2 tests on each edge, examined at several densities (FDR correction for multiple comparisons), determined whether the outcome groups differed in terms of edge presence, thereby highlighting the specific edges contributing to any elevation in hubness.

Lastly, we tested whether these hubness measures could successfully predict seizure outcome using a linear SVM classifier.[13] We tested 3 models separately, each containing the following variables: (1) selected hubness measures only, (2) demographic and clinical variables only (12 total: age, sex, handedness, verbal IQ, performance IQ, full-scale IQ, laterality of TLE, age at epilepsy onset, duration of epilepsy illness, seizure focality, interictal spike type, and type of temporal pathology evidenced by presurgical MRI scans), and (3) the variable sets of 1 and 2 combined. The prediction accuracy was estimated with 3 cross-validation methods, leave-one-out, 7-fold (10,000 permutations), and split sample (10,000 permutations), to ensure the independence between training and testing samples. For each selected hubness measure, we averaged the values over all the densities to avoid an arbitrary reliance on a single connection density.[24] To avoid the unequal sample size bias, we also repeated the above prediction analyses using a sample pool composed of all 21 NSF and 21 randomly selected SF patients with the same cross-validations.

RESULTS **Demographic and clinical characteristics.** There was no significant difference between the experimental groups in age, sex, or handedness ($p > 0.05$, table 1). In addition, the SF and NSF groups displayed no significant difference in any clinical characteristics listed in table 1 ($p > 0.05$).

Network properties comparison. The SF and NSF groups showed no differences in BC for any node at any density ($p > 0.05$). Compared to the SF group, however, the NSF group produced significantly higher DC and EC values, specifically involving the ipsilateral and contralateral thalami, across several

densities ($p < 0.05$, figure 1). In detail, the SF patients had DC and EC values essentially equivalent to those of the HCs, while the NSF patients showed significantly higher DC and EC values than the HCs. No significant difference was found in other regions after FDR correction (subtle differences at uncorrected $p < 0.05$ are reported in figure e-1).

These data indicate abnormally elevated hubness in the thalamus, reflective of greater connectivity (i.e., communication) importance in the NSF patients. To better elucidate these findings, we explored our data further through the following 3 steps.

First, we tested the importance of the thalamus to whole-brain network integration. While the E_{global} of the SF and NSF patients did not differ, both patient groups showed higher values than HCs across several densities ($p < 0.05$, asterisks in figure 2A), similar to previous findings.[25] After removing bilateral thalamic nodes/edges, we found a significant decline of E_{global} in all 3 groups ($p < 0.05$, plus signs in figure 2A), most dramatically in the NSF group ($p < 0.05$, figure 2B), indicating that these thalamic nodes played a greater role in whole-brain network integration in the NSF patients.

Second, we tested whether this hubness increase could be attributed to connections with the ictal-temporal lobe. After all the ictal-temporal nodes/edges were removed, the NSF group still displayed elevated DC and EC values in both thalami ($p < 0.05$, figure e-2), indicating that the connections responsible for the increased hubness were mainly extratemporal in nature.

Third, we investigated the connectivity between each thalamus and the remaining 89 nodes. Compared to SF patients, the NSF patients displayed extrathalamic connections in several regions across several densities. For instance, the ipsilateral thalamus was more frequently connected to 2 ipsilateral (anterior cingulum and superior temporal gyrus), and 6 contralateral (anterior cingulum, rolandic operculum, caudate, fusiform gyrus, and middle and superior temporal gyrus) regions ($p < 0.05$, figure 3A). The contralateral thalamus was more frequently connected to one ipsilateral (superior parietal gyrus) and 5 contralateral (caudate, supramarginal gyrus, middle occipital gyrus, cuneus, and rectus gyrus) regions ($p < 0.05$, figure 3B). Clearly, in the NSF group, both thalami display more connections with

Figure 1 **Comparisons of degree and eigenvector centrality at both ipsilateral (A) and contralateral (B) thalamus nodes**

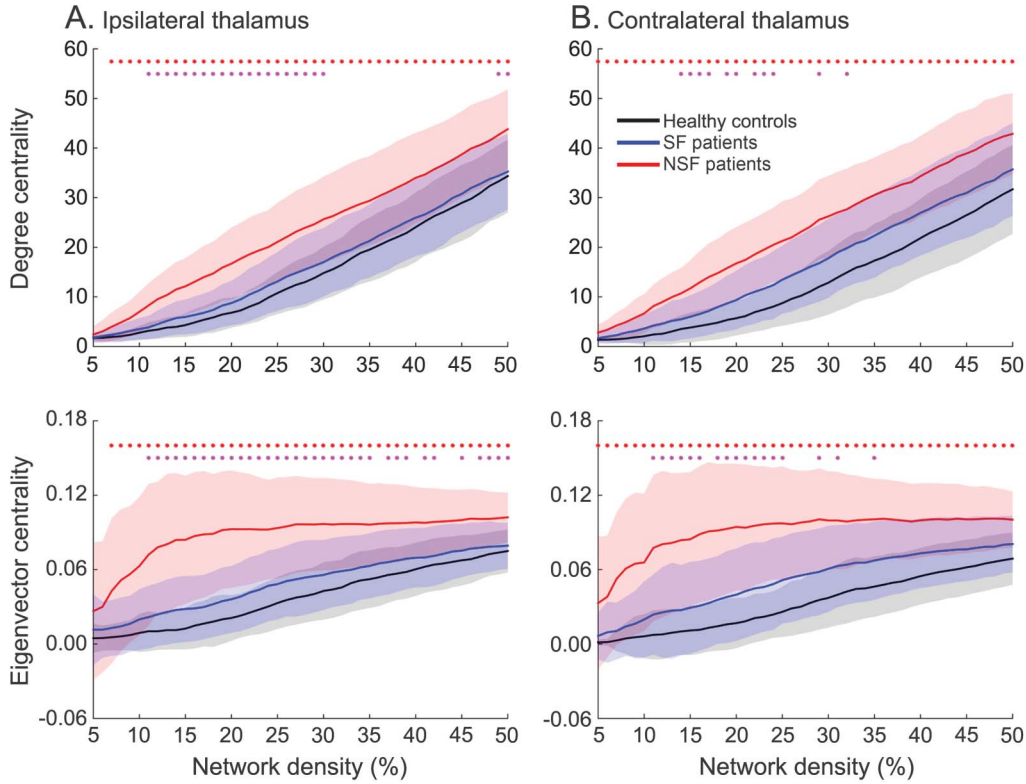

Red asterisks indicate significant differences (Welch permutation *t* tests, $p < 0.05$, FDR corrected) between the NSF patient and control groups; magenta asterisks indicate significant differences (Welch permutation *t* tests, $p < 0.05$, FDR corrected) between the NSF and SF patient groups. Shaded bands reflect SD. FDR = false discovery rate; NSF = not seizure-free; SF = seizure-free.

Figure 2 Comparisons of global efficiency

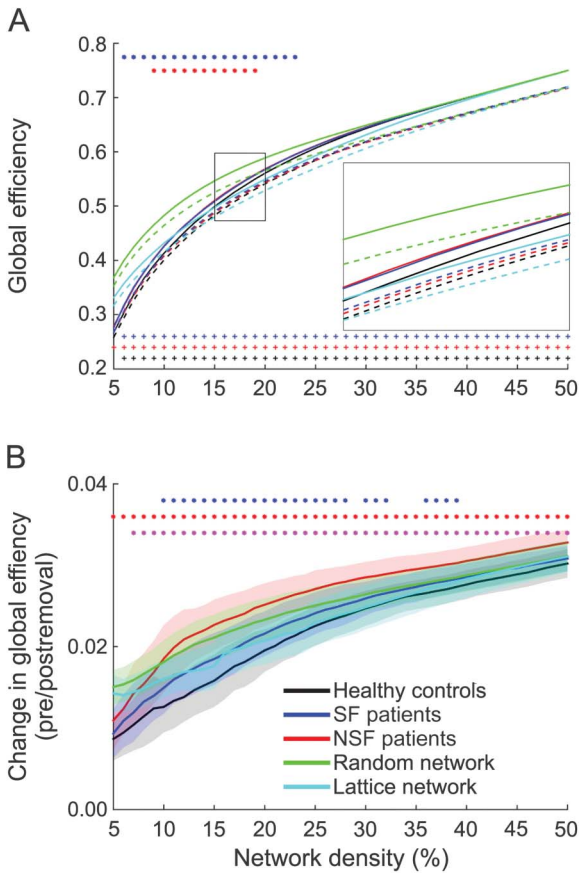

(A) Global efficiency before (solid line) and after (dash line) simulation of thalamus removal. Asterisks indicate significant differences (Welch permutation *t* tests, $p < 0.05$, FDR corrected) of initial global efficiency, with blue indicating SF patient vs control group and red indicating NSF patient vs control group. Plus signs indicate significant decline (Welch permutation *t* tests, $p < 0.05$, FDR corrected) in global efficiency, with blue, red, and black showing decline in SF and NSF patient groups and control group, respectively. (B) Comparisons of change in global efficiency. Asterisks indicate significant differences (Welch permutation *t* tests, $p < 0.05$, FDR corrected), with blue showing SF patient vs control group, red showing NSF patient vs control group, and magenta showing SF vs NSF patient group. Random and lattice networks before (solid line) and after (dash line) simulation of thalamus removal are also presented as references. Shaded bands reflect SD. FDR = false discovery rate; NSF = not seizure-free; SF = seizure-free.

the contralateral than the ipsilateral hemisphere. In contrast, no node in the SF group showed a heightened proportion of thalamic connections ($p > 0.05$).

On the basis of above results, we built SVM models with these 4 thalamic hubness measures. These models successfully predicted surgical outcome (75.55%), outperforming models built solely with demographic and clinical characteristics (58.12%). Moreover, adding later variables to the thalamic hubness models did not enhance predictive accuracy (71.40%). In addition, predictive models tested with equal-size samples yielded comparable results, demonstrating that the advantage of the thalamic hubness models was not due to a bias in sample ratios (table 2).

DISCUSSION In this study, we showed that specific hubness measures of brain organization can identify abnormal hubs, potentially reflecting cores of an epileptogenic network, with such presurgical measures associated with postoperative seizure recurrence and therefore reliably predictive of surgical outcomes. More specifically, compared to both SF patients and HCs, the NSF group displayed increased DC and EC in both ipsilateral and contralateral thalami. Simulating removal of thalamic nodes/edges reduced the E_{global} in all groups, most dramatically in the NSF group, revealing that in the context of poor seizure control, these thalamic hubs are of great importance, influencing the nature of whole-brain integration. Moreover, after removal of all the ictal-temporal nodes/edges, mimicking the effects of surgery, the same elevation in thalamic hubness values was obtained. Notably, the NSF patients displayed an increased number of thalamic connections, linking the bilateral thalami to several regions, mostly distributed in the contralateral hemisphere. Accordingly, these data suggest that a widespread epileptogenic network involving extratemporal regions, with the thalamus as hub, was clearly established in these patients before surgery, a network that could readily support seizure recurrence.

TLE is associated with a redistribution of hubness.[26,27] Previous studies have suggested that the global network properties (e.g., integration) are more disrupted[27] and more vulnerable[28] to the deletion of major hubs in patients with unfavorable outcomes. Our data demonstrate that one such crucial hub could be the bilateral thalami. Patients with TLE who show higher levels of functional synchronization between the thalamus and other extratemporal regions presurgically may be developing a form of occult epileptogenic signaling, setting the stage for postoperative seizure recurrence.

The thalamus is well recognized for its crucial role in the generation and spread of seizures.[29] Spared in ATL, it could support recurrent seizures postoperatively.[8,11] For instance, patients with persistent seizures have greater white matter abnormalities in thalamo-temporal tracts,[11,12] more disrupted right thalamo-hippocampus rsFC,[30] and higher thalamo-temporal coupling,[31] all indicating that interaction between the thalamus and ictal-temporal lobe can, after surgery, increase seizure burden and predispose toward seizure propagation. Our findings suggest that the importance of the thalamus to seizure recurrence emerges not just because of its prior connections to the ictal-temporal lobe, the region removed by ATL, but also because of its connections to extratemporal regions, which are spared by ATL and likely form the key parts of postsurgical epileptogenic networks. Thus, our data are consistent with prior evidence showing that the thalamus is crucial to seizure recurrence after surgery but clarify its role as a hub of potential epileptogenic networks involving primarily

Figure 3 Thalamic edges showing different percentile of existence between SF and NSF patients

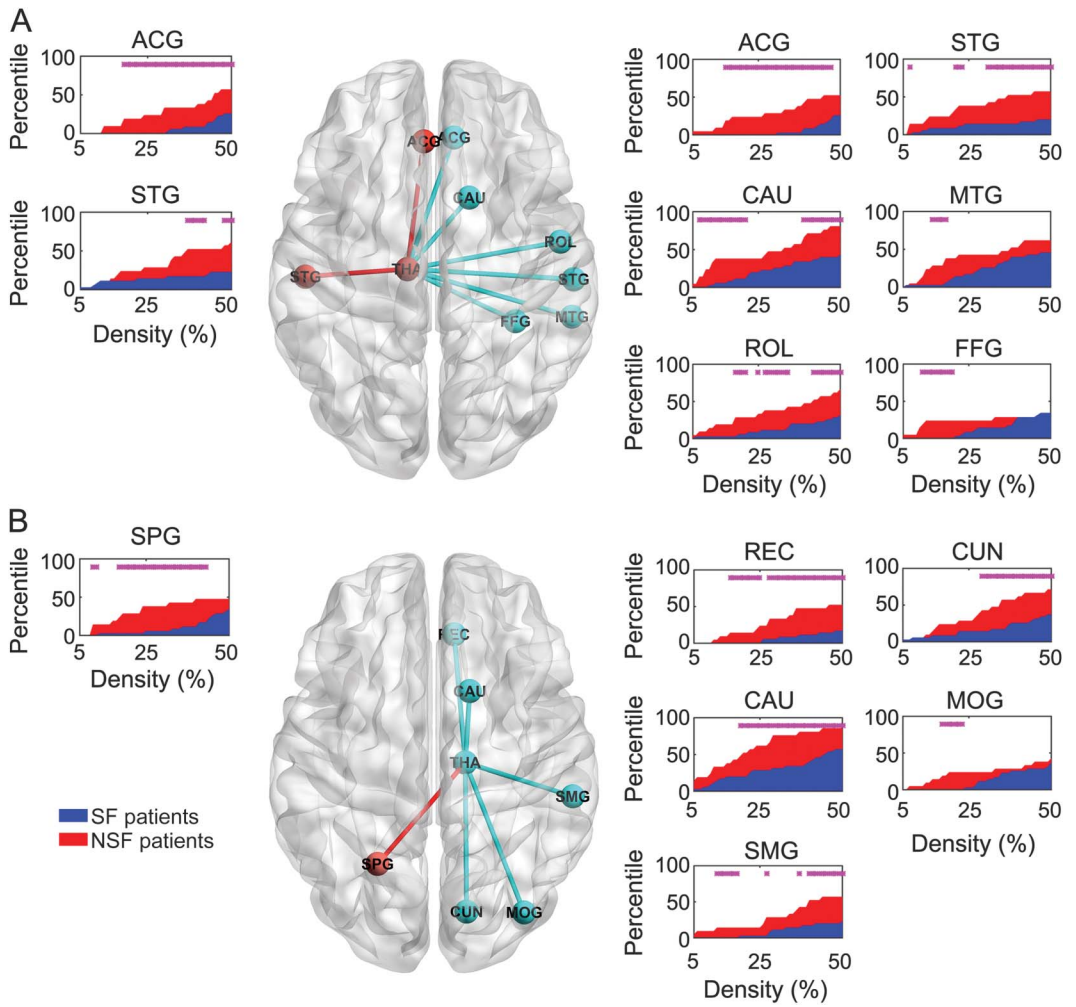

Nodes and edges located in the ipsilateral hemisphere are shown in red; nodes and edges located in the contralateral hemisphere are shown in cyan. Blue area reflects the percentile of existence of each edge across a series of network densities (5%–50%) in the SF patient group; Red area reflects the percentile of existence of each edge across a series of network densities (5%–50%) in the NSF patient group. Magenta asterisk indicates significant differences (χ^2 tests, $p < 0.05$, FDR corrected) between the SF and NSF patient groups. (A) Ipsilateral thalamic edges. (B) Contralateral thalamic edges. ACG = anterior cingulum; CAU = caudate; CUN = cuneus; FDR = false discovery rate; FFG = fusiform gyrus; MOG = middle occipital gyrus; MTG = middle temporal gyrus; NSF = not seizure-free; REC = rectus gyrus; ROL = rolandic operculum; SF = seizure-free; SMG = supramarginal gyrus; SPG = superior parietal gyrus; STG = superior temporal gyrus.

the contralateral hemisphere, although also including ipsilateral regions spared by ATL (posterior superior temporal gyrus). Unlike pathologies such as epileptogenic temporal residue, which can be treated with a second resection, this contralateral thalamic network is not subject to such treatment. Rather than suggesting further resections, our findings help set the stage for alternative interventions such as brain electric stimulation. For example, the implication of targeting the bilateral thalami is exactly in accord with general strategies behind some current investigative trials (i.e., Stimulation of the Anterior Nucleus of Thalamus for Epilepsy [SANTE][32]).

A practical challenge is to identify the full epileptogenic network(s) that are capable of supporting seizures after surgery. Part of the difficulty is that these at-risk regions can vary across individuals. Our data show how topologic brain organization information may constitute an important starting point. For instance, we observed some thalamocortical connections to be more prevalent than others (depicted in figure 3) in our sample; however, thalamic hubness was neither dependent on nor specific to any connection. This means that the thalamus could connect to completely different regions in other NSF patients yet still maintain elevated hubness levels.

To demonstrate reproducibility, we repeated our analysis using the Harvard-Oxford Atlas and produced nearly identical results (figure e-3), providing

Table 2 Surgical outcome prediction summary

	Full original sample, %					Equal-sized sample, %[a]				
	ACC	SEN	SPC	PPV	NPV	ACC	SEN	SPC	PPV	NPV
Thalamic hubness measures										
Leave-one-out	76.79	85.71	61.90	78.95	72.22	70.98	76.05	65.92	68.97	73.68
7-Fold[a]	75.85	85.79	59.26	77.84	71.71	71.57	76.93	66.21	69.45	74.46
Split sample[a]	74.00	84.77	56.03	76.31	69.53	70.95	73.26	67.14	69.09	71.89
Mean	75.55	85.42	59.06	77.70	71.15	71.17	75.41	66.42	69.17	73.34
Demographic and clinical characteristics										
Leave-one-out	60.71	74.29	38.10	66.67	47.06	48.31	46.30	50.33	48.27	48.32
7-Fold[a]	59.24	73.93	34.75	65.40	44.51	49.55	48.47	50.63	49.54	49.54
Split sample[a]	54.40	67.56	32.46	62.47	37.49	48.62	46.19	51.16	48.34	48.72
Mean	58.12	71.93	35.10	64.85	43.02	48.83	46.99	50.71	48.72	48.86
Thalamic hubness measures + demographic and clinical characteristics										
Leave-one-out	75.00	82.86	61.90	78.38	68.42	62.13	63.44	60.82	61.73	62.71
7-Fold[a]	71.48	79.97	57.34	75.79	63.45	63.15	64.36	61.94	62.83	63.74
Split sample[a]	67.73	75.67	54.51	73.64	58.02	61.49	58.32	63.52	61.60	60.88
Mean	71.40	79.50	57.92	75.94	63.30	62.26	62.04	62.09	62.05	62.44
Null model	62.50	100	0	62.50	NA	50.00	100	0	50.00	NA

Abbreviations: ACC = accuracy; NPV = negative predictive value; PPV = positive predictive value; SEN = sensitivity; SPC = specificity.
Full original sample: training and testing samples for cross-validation were generated by splitting the full sample pool (56), maintaining the original seizure-free/not seizure-free outcome ratio of 5:3. Equal-sized sample: training and testing samples for cross-validation were generated by splitting a selective sample pool (42) constituted by the 21 not seizure-free patients and 21 randomly selected seizure-free patients, establishing a seizure-free/not seizure-free outcome ratio of 1:1.
[a] Run with 10,000 permutations.

strong evidence of robustness and reliability. Another methodological consideration was our choice of binary instead of weighted graphs as a way of being more selective about the source of nodal hubness (i.e., in weighted graphs, higher hubness can come from extra edges, a stronger correlation between edges, or both; in binary graphs, high hubness emerges solely from extra edges). Nevertheless, to further verify robustness, we retested our data with weighted graphs and obtained similar results. Namely, the NSF patients exhibited both higher nodal strength (weighted version of DC) and higher EC involving the bilateral thalami (figure e-4).

Currently, the best neuroimaging predictors of seizure outcome involve primarily ipsilateral-temporal features extracted with structural approaches (e.g., morphology of mesial temporal structures,[33] ipsilateral-temporal white matter connections[12]), yielding prediction strengths on the order of 80%[12] to 90%.[33] Our study demonstrates that extratemporal features such as thalamic hubness measures extracted from rsFC can also serve as successful predictors. As an alternative perspective, rsFC reflects structural connectivity[34] and can be inferred from structural connectivity.[35] Furthermore, it provides sensitivity to long-range interregional communication supported only by indirect physiologic links.[36] The validity of rsFC comes from its association with human behavior[14] and ability to uniquely characterize neurologic and psychiatric disease.[37,38] As a demonstration, we found that SVM models trained with <30 cases (in case of split sample) using rsFC features (thalamic hubness) can readily predict seizure outcome in a set of independent patients at 74% accuracy, exceeding the predictive value of models with solely clinical characteristics.

In NSF patients, the thalamic nodes showed enriched connections (higher DC), and the targets of these connections were themselves highly connected (other hubs, higher EC). However, these additional connections are not geodesic in nature (not the shortest pathway between 2 other nodes, i.e., no reliable effects of BC) and hence do not bring additional efficiency to information flow, which may reflect a maladaptive, pathologic process driving seizure recurrence.

Our project has several limitations. The representativeness of our sample could be biased because of its limited size. In addition, seizure outcome varies over time; hence, the predictive value of presurgical thalamic hubness against longer-term outcome remains

to be explored. For instance, the brain could potentially reorganize over time in ways that may or may not support seizure freedom. In terms of methods, the coherence of regional signal change could be influenced by noise such as head motion. To address this, we used a higher-order head motion nuisance regression model[39] and a maximal overlap discrete wavelet transform procedure to remove the signal components associated with head motion and physiologic noise outside our band of interest. We also acknowledge that rsfMRI covers only a limited range of signal frequency, while different network dynamics at other frequencies, especially high frequencies,[40] need to be explored. Lastly, because we did not collect simultaneous EEG during our scan, we cannot completely rule out the existence of interictal activity at the time of data collection, although any such interictal activity would not have been consistent across patients, thereby canceling out any systematic correlation with our findings.

The thalamic hubness our data highlight provides clues for developing strategies beyond just ATL, with an eye toward additional or alternative targeted interventions. Our data also have relevance for the prediction of surgical outcomes, outperforming the clinical characteristics commonly used in epilepsy surgical centers.

AUTHOR CONTRIBUTIONS

Xiaosong He: study design, acquisition, analysis and interpretation of data, drafting the manuscript. Gaelle E. Doucet: acquisition data, revising the manuscript for intellectual content. Dorian Pustina: acquisition and analysis of data, revising the manuscript for intellectual content. Michael R. Sperling: diagnosing/treating the patients, revising the manuscript for intellectual content. Ashwini D. Sharan: operating on the patients, revising the manuscript. Joseph I. Tracy: study design, interpretation of data, critical revision of manuscript for intellectual content.

ACKNOWLEDGMENT

The authors thank all the HCs and patients with epilepsy, kept anonymous, who provided data for this study. The authors also thank the 4 anonymous reviewers for their suggestions to improve this manuscript.

STUDY FUNDING

No targeted funding reported.

DISCLOSURE

X. He, G. Doucet, and D. Pustina report no disclosures relevant to the manuscript. M. Sperling reports research contracts as principal investigator through Thomas Jefferson University from UCB Pharma, Eisai, Sunovion, SK Life Sciences, Glaxo, Marinus Pharmaceuticals, Accorda, Lundbeck, Pfizer, Neurelis, Medtronic, Brain Sentinel, and Upsher Smith, as well as research support from DARPA and the NIH through Thomas Jefferson University. He has consulted for Medtronic through Thomas Jefferson University and for Medscape for continuing medical education program development. A. Sharan serves on the advisory board for Medtronic, is a speaker for St. Jude Medical, receives grant support from St. Jude Medical, is the owner of Integrated Care Pharmacy, and is the founder of ICVrx, a company developing drug delivery technologies for epilepsy. J. Tracy reports no disclosures relevant to the manuscript. Go to Neurology.org for full disclosures.

Received October 26, 2016. Accepted in final form March 14, 2017.

REFERENCES

1. Sperling MR, O'Connor MJ, Saykin AJ, Plummer C. Temporal lobectomy for refractory epilepsy. JAMA 1996;276:470–475.
2. Wiebe S, Blume WT, Girvin JP, Eliasziw M; Effectiveness, Efficiency of Surgery for Temporal Lobe Epilepsy Study Group. A randomized, controlled trial of surgery for temporal-lobe epilepsy. N Engl J Med 2001;345:311–318.
3. Spencer S, Huh L. Outcomes of epilepsy surgery in adults and children. Lancet Neurol 2008;7:525–537.
4. Asadi-Pooya AA, Nei M, Sharan A, Sperling MR. Historical risk factors associated with seizure outcome after surgery for drug-resistant mesial temporal lobe epilepsy. World Neurosurg 2016;89:78–83.
5. Asadi-Pooya AA, Nei M, Sharan A, Sperling MR. Patient historical risk factors associated with seizure outcome after surgery for drug-resistant nonlesional temporal lobe epilepsy. World Neurosurg 2016;91:205–209.
6. de Tisi J, Bell GS, Peacock JL, et al. The long-term outcome of adult epilepsy surgery, patterns of seizure remission, and relapse: a cohort study. Lancet 2011;378:1388–1395.
7. Ryvlin P. Beyond pharmacotherapy: surgical management. Epilepsia 2003;44(suppl):23–28.
8. Keller SS, Richardson MP, O'Muircheartaigh J, Schoene-Bake JC, Elger C, Weber B. Morphometric MRI alterations and postoperative seizure control in refractory temporal lobe epilepsy. Hum Brain Mapp 2015;36:1637–1647.
9. Doucet GE, He X, Sperling M, Sharan A, Tracy JI. Frontal gray matter abnormalities predict seizure outcome in refractory temporal lobe epilepsy patients. NeuroImage Clin 2015;9:458–466.
10. Bernhardt BC, Bernasconi N, Concha L, Bernasconi A. Cortical thickness analysis in temporal lobe epilepsy: reproducibility and relation to outcome. Neurology 2010;74:1776–1784.
11. Keller SS, Richardson MP, Schoene-Bake JC, et al. Thalamotemporal alteration and postoperative seizures in temporal lobe epilepsy. Ann Neurol 2015;77:760–774.
12. Bonilha L, Jensen JH, Baker N, et al. The brain connectome as a personalized biomarker of seizure outcomes after temporal lobectomy. Neurology 2015;84:1846–1853.
13. Munsell BC, Wee CY, Keller SS, et al. Evaluation of machine learning algorithms for treatment outcome prediction in patients with epilepsy based on structural connectome data. Neuroimage 2015;118:219–230.
14. Fox MD, Raichle ME. Spontaneous fluctuations in brain activity observed with functional magnetic resonance imaging. Nat Rev Neurosci 2007;8:700–711.
15. Wasserman S, Faust K. Social Network Analysis: Methods and Applications. Cambridge: Cambridge University Press; 1994.
16. Tracy JI, Dechant V, Sperling MR, Cho R, Glosser D. The association of mood with quality of life ratings in epilepsy. Neurology 2007;68:1101–1107.
17. Engel J Jr, Wiebe S, French J, et al. Practice parameter: temporal lobe and localized neocortical resections for epilepsy: report of the Quality Standards Subcommittee of the American Academy of Neurology, in association with the American Epilepsy Society and the American Association of Neurological Surgeons. Neurology 2003;60:538–547.
18. Tzourio-Mazoyer N, Landeau B, Papathanassiou D, et al. Automated anatomical labeling of activations in SPM

using a macroscopic anatomical parcellation of the MNI MRI single-subject brain. Neuroimage 2002;15:273–289.
19. Percival DB, Walden AT. Wavelet Methods for Time Series Analysis. Cambridge: Cambridge University Press; 2006.
20. Lo CY, Su TW, Huang CC, et al. Randomization and resilience of brain functional networks as systems-level endophenotypes of schizophrenia. Proc Natl Acad Sci USA 2015;112:9123–9128.
21. Alexander-Bloch AF, Gogtay N, Meunier D, et al. Disrupted modularity and local connectivity of brain functional networks in childhood-onset schizophrenia. Front Syst Neurosci 2010;4:147.
22. Rubinov M, Sporns O. Complex network measures of brain connectivity: uses and interpretations. Neuroimage 2010;52:1059–1069.
23. Smith SM, Jenkinson M, Woolrich MW, et al. Advances in functional and structural MR image analysis and implementation as FSL. Neuroimage 2004;23(suppl): S208–S219.
24. Bassett DS, Bullmore E, Verchinski BA, Mattay VS, Weinberger DR, Meyer-Lindenberg A. Hierarchical organization of human cortical networks in health and schizophrenia. J Neurosci 2008;28:9239–9248.
25. Song J, Nair VA, Gaggl W, Prabhakaran V. Disrupted brain functional organization in epilepsy revealed by graph theory analysis. Brain Connect 2015;5:276–283.
26. Liao W, Zhang Z, Pan Z, et al. Altered functional connectivity and small-world in mesial temporal lobe epilepsy. PLoS One 2010;5:e8525.
27. Bernhardt BC, Chen Z, He Y, Evans AC, Bernasconi N. Graph-theoretical analysis reveals disrupted small-world organization of cortical thickness correlation networks in temporal lobe epilepsy. Cereb Cortex 2011;21: 2147–2157.
28. Liao W, Ji GJ, Xu Q, et al. Functional connectome before and following temporal lobectomy in mesial temporal lobe epilepsy. Sci Rep 2016;6:23153.
29. Blumenfeld H. The thalamus and seizures. Arch Neurol 2002;59:135–137.
30. Morgan VL, Sonmezturk HH, Gore JC, Abou-Khalil B. Lateralization of temporal lobe epilepsy using resting functional magnetic resonance imaging connectivity of hippocampal networks. Epilepsia 2012;53:1628–1635.
31. Guye M, Regis J, Tamura M, et al. The role of corticothalamic coupling in human temporal lobe epilepsy. Brain 2006;129:1917–1928.
32. Fisher R, Salanova V, Witt T, et al. Electrical stimulation of the anterior nucleus of thalamus for treatment of refractory epilepsy. Epilepsia 2010;51:899–908.
33. Bernhardt BC, Hong SJ, Bernasconi A, Bernasconi N. Magnetic resonance imaging pattern learning in temporal lobe epilepsy: classification and prognostics. Ann Neurol 2015;77:436–446.
34. Greicius MD, Supekar K, Menon V, Dougherty RF. Resting-state functional connectivity reflects structural connectivity in the default mode network. Cereb Cortex 2009;19:72–78.
35. Honey CJ, Sporns O, Cammoun L, et al. Predicting human resting-state functional connectivity from structural connectivity. Proc Natl Acad Sci USA 2009;106: 2035–2040.
36. Damoiseaux JS, Greicius MD. Greater than the sum of its parts: a review of studies combining structural connectivity and resting-state functional connectivity. Brain Struct Funct 2009;213:525–533.
37. Zhang D, Raichle ME. Disease and the brain's dark energy. Nat Rev Neurol 2010;6:15–28.
38. Fornito A, Zalesky A, Breakspear M. The connectomics of brain disorders. Nat Rev Neurosci 2015;16:159–172.
39. Friston KJ, Williams S, Howard R, Frackowiak RS, Turner R. Movement-related effects in fMRI time-series. Magn Reson Med 1996;35:346–355.
40. Zijlmans M, Jiruska P, Zelmann R, Leijten FS, Jefferys JG, Gotman J. High-frequency oscillations as a new biomarker in epilepsy. Ann Neurol 2012;71:169–178.